Published in final edited form as:
Pharm Res. 2013 April ; 30(4): 1099–1109. doi:10.1007/s11095-012-0946-7.

Transdermal Delivery of Molecules is Limited by Full Epidermis, Not Just Stratum Corneum

Samantha N. Andrews[1], **Eunhye Jeong**[2], and **Mark R. Prausnitz**[1,2,*]

[1]Wallace Coulter Department of Biomedical Engineering, Georgia Institute of Technology, Atlanta, GA, USA 30332

[2]School of Chemical and Biomolecular Engineering, Georgia Institute of Technology, Atlanta, GA, USA 30332

Abstract

Purpose—Most methods to increase transdermal drug delivery focus on increasing stratum corneum permeability, without addressing the need to increase permeability of viable epidermis. Here, we assess the hypothesis that viable epidermis offers a significant permeability barrier that becomes rate limiting upon sufficient permeabilization of stratum corneum.

Methods—We tested this hypothesis by using calibrated microdermabrasion to selectively remove stratum corneum or full epidermis in pig and human skin, and then measuring skin permeability to a small molecule (sulforhodamine) and macromolecules (bovine serum albumin, insulin, inactivated influenza vaccine) in vitro.

Results—We found that removal of stratum corneum dramatically increased skin permeability to all compounds tested. However, removal of full epidermis increased skin permeability by another 1 – 2 orders of magnitude. We also studied the effects of removing skin tissue only from localized spots on the skin surface by covering skin with a mask containing 125-μm holes during tissue removal. Skin permeabilized in this less- invasive way showed similar results. This suggests that microdermabrasion of skin using a mask may provide an effective way to increase skin permeability.

Conclusions—We conclude that viable epidermis offers a significant permeability barrier that becomes rate limiting upon removal of stratum corneum.

Keywords

stratum corneum; viable epidermis; skin; transdermal drug delivery; microdermabrasion; insulin

INTRODUCTION

Transdermal delivery is an attractive route of drug administration due to the skin's large surface area and ease of administration (1). Further advantages are that it avoids drug degradation due to the first pass effect of the liver, does not involve the use of needles, and does not cause pain. However, the skin serves as a barrier that protects the body from the

*To whom all correspondence should be addressed. Corresponding author: Mark R. Prausnitz School of Chemical and Biomolecular Engineering Georgia Institute of Technology 311 Ferst Drive Atlanta, GA 30332-0100 USA Ph: +1 404 894 5135 Fax: +1 404 894 2291 prausnitz@gatech.edu.

This potential conflict of interest has been disclosed and is being managed by the Georgia Institute of Technology and Emory University.

external environment and prevents water loss. This barrier function also prevents most hydrophilic and large molecular weight drugs (>500 Da) from penetrating intact skin.

The main barrier to transdermal drug delivery is the stratum corneum, the top layer of skin. The stratum corneum measures 10 – 15 μm thick and is composed of dead flattened corneocytes that are surrounded by a lipid extracellular matrix (2). Below is the viable epidermis, which is a cellular, avascular tissue measuring 50 – 100 μm thick. The stratum corneum and viable epidermis together comprise the full epidermis. There is a basement membrane at the base of the epidermis and there is recent evidence for the existence of tight junctions in the viable epidermis (3), both of which may offer resistance to transport of molecule across the epidermis. Deeper still is the dermis, which is largely a fibrous tissue measuring 1 – 2 mm thick. There is a rich capillary bed in the superficial dermis just below the epidermis, which is the primary site of drug update into systemic circulation. Thus, successful transdermal drug delivery typically involves drug transport across the epidermis to the superficial dermal capillary bed.

Because the stratum corneum is the greatest barrier to transport, most methods to increase transdermal drug delivery have emphasized increasing stratum corneum permeability. Chemical enhancers disorganize or extract intercellular lipids of the stratum corneum (4, 5), where recent approaches have involved designing formulations (6) or biochemical methods (7) that specifically target stratum corneum lipids. Ultrasound uses cavitation to disrupt stratum corneum lipids (8) and various other physical methods, including microneedles, thermal ablation and microdermabrasion, create micron-scale holes in the stratum corneum to increase permeability (9).

Until recently, methods to increase stratum corneum permeability were generally not effective enough to make the stratum corneum so permeable that the barrier posed by the viable epidermis mattered. However, that has now changed with the development of various physical methods and highly optimized chemical formulations, such that we need to revisit the permeability of the full epidermis and not focus only on stratum corneum. This study therefore tests the hypothesis that viable epidermis offers a significant permeability barrier to both small molecules and macromolecules that becomes the rate limiting step upon sufficient permeabilization of the stratum corneum.

Stated another way, this study seeks to determine if transdermal delivery strategies should seek to selectively increase stratum corneum permeability or if they should be designed to increase the permeability of the full epidermis. Should thermal ablation and microdermabrasion devices remove just stratum corneum or should they make holes that fully cross the epidermis? Should microneedles be optimally designed to puncture just across the stratum corneum or would they be more effective if they crossed the full epidermis? Are chemical and physical methods that target stratum corneum inherently limited in their ability to increase transdermal delivery because they do not also affect the barrier properties of viable epidermis?

To provide insight into these questions, we used calibrated microdermabrasion to selectively remove either stratum corneum alone or the full epidermis and then assessed skin permeability. Microdermabrasion is a non-invasive, FDA-approved cosmetic technique that is used to reduce the appearance of superficial scars and wrinkles (10–12). The procedure removes skin tissue by bombarding it with abrasive particles under vacuum (13, 14). Although the procedure was originally designed for cosmetic use, researchers have used microdermabrasion to increase skin permeability by partial or complete removal of stratum corneum (15–18).

To provide more controlled tissue removal, we previously studied the effects of microdermabrasion operating conditions on tissue removal from the skin (19). We optimized conditions that remove stratum corneum alone, without significant removal of viable epidermis, and other conditions that remove the full epidermis. We have used these optimized conditions in the present study to compare skin permeability after removal of stratum corneum alone versus removal of full epidermis.

MATERIALS AND METHODS

Porcine skin experiments (without a mask)

Abrasion Protocol—All microdermabrasion experiments without the use of a polymer mask were conducted on excised full-thickness adult feeder porcine dorsal skin (2–9 month old, average weight 32 kg, Pel-freeze Biologicals, Rogers, AR) using a Gold Series MegaPeel microdermabrasion machine (DermaMed USA, Lenni, PA) with the gold handpiece assembly. The subcutaneous fat was removed with a scalpel, although a thin layer of the subcutaneous tissue remained adherent, and the hair was shaved with surgical prep razors (Medex Supply, Monsey, NY) prior to the experiment. The abrasion area was bounded by a window cut out of a piece of rectangular adhesive foam (the window measured 41 mm by 15 mm) applied to the skin and the microdermabrasion handpiece was moved along the skin within the window in the adhesive foam at a constant speed of 1 pass/s at suction pressures and crystal flow rates described below. Animal tissue used in this way was classified as exempt from review by the Georgia Tech Institutional Animal Care and Use Committee.

Sulforhodamine Delivery—Sulforhodamine B (Invitrogen, Carlsbad, CA), a red-fluorescent molecule, was used as a low-molecular weight, hydrophilic drug model. Its molecular weight is 558.6 Da. The delivery experiments were carried out by abrading the skin at two vacuum pressures, −25 and −45 kPa, for 10 and 50 passes each. The crystal flow rate was set to 4.5 turns of the crystal flow rate knob (which corresponds to 0.36 g/s of crystals (19)). After abrasion, the treated skin and an untreated control were placed in horizontal diffusion cells (PermeGear, Bethlehem, Pa) with a water jacket set to 37 °C. Three milliliters of 10^{-3} M sulforhodamine B (in PBS) and phosphate buffered saline (PBS, Sigma-Aldrich, St. Louis, MO) were added to the donor and receiver chambers, respectively. For histology experiments, the skin was exposed for 1, 6, or 24 h and then removed for examination. For quantitative skin permeability experiments, the flux of sulforhodamine across the skin over 12 h was quantified by emptying the receiving chamber solution every hour and measuring the fluorescence by calibrated spectrofluorimetry (Photon Technology International, Birmingham, NJ). Fresh PBS was added to the receiver chamber at each sampling point. Three replicates for each time point were carried out. At the conclusion of the experiments, the skin was embedded in Optimal Cutting Temperature Compound Sakura Finetek, Torrance, CA) and frozen using dry ice for histological analysis.

For the histological analysis, the skin was sectioned at 10 μm thickness using a Leica 3050S cryostat (Leica Microsystems, Wetzlar, Germany). The fluorescence was viewed using a Nikon 600E microscope (Nikon, Toyko, Japan) and pictures were collected using Qcapture camera and software (Q Imaging, Pleasanton, CA). Slides were also stained with routine hematoxylin and eosin using an autostainer (Leica Microsystems) and photographed. All skin samples for each compound were processed using the same histological process unless otherwise noted.

Bovine Serum Albumin Delivery—Texas Red-labeled bovine serum albumin (BSA, Invitrogen, Carlsbad, CA), a red-fluorescent-labeled protein, was used as a model compound

for protein delivery. BSA has a molecular weight of 66 kDa. The skin was abraded at a pressure of −50 kPa for 50 passes (1 pass/s) at a crystal flow rate of 4.5 turns of the knob (0.36 g/s) to remove the stratum corneum. The permeation of BSA across skin was studied in the same manner as sulforhodamine, except the skin was placed in vertical Franz cell diffusion chambers (PermeGear, Bethlehem, PA). The vertical Franz cells permitted the use of a smaller donor solution volume. The Franz cells were placed in a heating blocking (PermeGear) set to 37 °C. One hundred microliters of 10^{-5} M BSA (in PBS) and 5 mL of PBS were added to the donor and receiver chambers, respectively. The skin was exposed to BSA for 1, 6, and 24 h. The flux was not measured, since we determined in preliminary experiments that significant fluorescent signal was not detected in the receiver solution within 24 h from BSA permeating across the full-thickness pig skin used in this study. At the completion of the experiment, the skin was frozen for histological analysis, as described above.

Inactivated Influenza Virus Delivery—The model vaccine used for delivery was inactivated influenza virus; the molecular weight was ~3×10^6 Da (20). Influenza virus was conjugated to red-fluorescent R18 (octadecyl rhodamine B chloride) for fluorescent imaging. To conjugate R18 to the virus, 10 μL R18 (Invitrogen, Carlsbad, CA) was mixed with 200 μL of inactivated virus (3 mg/ml). The solution was incubated for 1 h at room temperature, then ultracentrifuged at 28,000×g for 1 h to remove unbound R18. After centrifugation, 1 mL of 20% sucrose, 9 mL PBS (without Ca or Mg), and 1 mL inactivated virus formulation (200 μL R-18 stained inactivated virus, 0.7 mL PBS, and 0.1 mL fetal bovine serum) were mixed and centrifuged. The supernatant was removed and 200 μL of PBS was added to resuspend the solution overnight at 4 °C. The abrasion settings and the diffusion experiments for inactivated influenza virus were conducted using the same abrasion and delivery protocol as the BSA experiment. Histology was used to assess the permeation depth. Due to its large molecular weight, the flux of virus was not measured quantitatively.

Human Skin Experiments (with a mask)

Sulforhodamine and insulin were delivered to excised split thickness human cadaver skin (National Disease Research Interchange, Philadelphia, PA) after microdermabrasion through a polymer mask. The skin was dermatomed to a thickness of 200 to 600 μm. Human tissue used in this way was classified as exempt from review by the Georgia Tech Institutional Review Board.

The mask was used to reduce the area of abrasion and allow better three-dimensional control of skin removal. The polymer masks were fabricated out of 70 μm-thick polyethylene terephthalate (McMaster Carr, Aurora, OH) and the holes (125 μm diameter) were laser cut with a Hermes LS500XL CO_2 laser (Gravograph, Duluth, GA).. This produced a polymer sheet with 408 holes each spaced 500 μm apart (center-to-center spacing) covering a total area of 0.95 cm^2.

The mask was adhered to the skin using tape along the sides of the mask and the skin was abraded using the conditions (i) −30 kPa at a crystal flow rate of 0.23 g/s (5 turns of the crystal flow rate knob) for 20 s to remove the stratum corneum and (ii) −50 kPa at a crystal flow rate of 0.95 g/s (0 turns of the crystal flow rate knob) for 60 s to remove the viable epidermis (19). There were also two negative controls: (i) skin exposed to the test molecule, but not abraded and (ii) skin that was abraded, but only exposed to PBS. Three replicates of each condition were used.

During microdermabrasion, the microdermabrasion tip was moved to multiple sites on the mask to maximize the area of abrasion. After abrasion, the pores were selectively stained

with green dye (McCormick & Co, Hunt Valley, MD) and photographed using an Olympus SZX12 stereoscope (Olympus, Tokyo, Japan) and Leica DC 300 camera (Leica Microsystems, Wetzlar, Germany), and analyzed using Adobe Photoshop software (Adobe Systems, San Jose, CA). All skin samples were then placed in vertical Franz cell diffusion chambers and the chambers were housed in a heating block set to 37 °C. At the conclusion of each delivery experiment, the area of abrasion was determined again using green dye and the skin was snap frozen in dry ice for histological analysis.

For the sulforhodamine delivery experiments, 200 μL of 10^{-3} M sulforhodamine B and 5 mL of PBS were added to the donor and receiver chambers, respectively. The donor chamber was covered with parafilm (Pechiney Plastic Packaging, Chicago, IL) to reduce evaporation. The receiver chamber was sampled every hour for 12 h by removing all of the liquid and replacing it with 5 mL of PBS at each time point. The sulforhodamine concentration in the receiver chamber was measured, using fluorescence, in the same manner as the sulforhodamine experiments in the previous section.

To measure insulin delivery, 100 μL of an insulin solution was added to the donor chamber. The insulin solution consisted of 80 μL of U-500 Humulin-R insulin (Eli Lilly, Indianapolis, IN) and 20 μL of 2.5 mg/ml FITC-labeled bovine insulin (Sigma-Aldrich). The bovine insulin was used to visualize insulin transport during the histological analysis. The receiver chamber contained 5 mL of PBS mixed with 10^{-2} M sodium azide (Sigma-Aldrich), a preservative. The donor chamber was covered with parafilm and the donor solution was replaced at each sampling time due to possible instability of the insulin. The receiver chamber was sampled every 6 h for 54 h in the same manner as the sulforhodamine experiments.

The concentration of the FITC-labeled bovine insulin was measured using fluorescence using the same protocol as the sulforhodamine experiments. The total insulin concentration in the receiver chamber solution was additionally quantified using a rat insulin enzyme-linked immunoassay (ELISA) kit (Alpco Diagnostics, Salem, NH), which had cross-reactivity with the Humulin insulin used in this study. The assay was carried out according to the manufacturer's protocol.

RESULTS

Skin Permeability After Removal of Stratum Corneum in Pig Skin

We first identified microdermabrasion conditions that selectively removed different amounts of skin tissue, guided by our previous work that studied this in detail (19). Fig. 1A shows intact pig skin, with pink-stained stratum corneum on top, purple-stained viable epidermis below, and lightly stained dermis at the bottom. In Fig. 1B, the skin was exposed to microdermabrasion at mild conditions (−45 kPa, 10 passes), which removed part of the stratum corneum, but not all of it. Fig. 1C shows the effects of more aggressive microdermabrasion (−45 kPa, 50 passes), which fully removed the stratum corneum, but left the viable epidermis intact.

Permeation of Sulforhodamine B—Our first experiments sought to validate the role of stratum corneum as a major barrier to transport of molecules, and that removal of stratum corneum enables delivery of a small, hydrophilic molecule (discussed here) and of macromolecules (discussed below). The skin was therefore exposed to sulforhodamine for up to 24 h and then examined histologically to image the depth of penetration of the molecule. Figs. 1D – 1F show representative images of intact (unabraded) skin over time. The pictures were taken at the same exposure time and gain to allow comparison of the depth and intensity of the sulforhodamine at each time point on the same basis. Very little

sulforhodamine permeated into the skin during the 24-h experiment, indicating the good barrier properties of the stratum corneum.

In Figs. 1G – 1I, the skin was microdermabraded under conditions that fully removed stratum corneum. In this case, sulforhodamine permeated much more rapidly and deeply into the skin, because the stratum corneum barrier was removed. We conducted additional experiments at milder microdermabrasion conditions that only partially removed the stratum corneum, which also increased permeation of sulforhodamine into the skin, but to a lesser extent than after full stratum corneum removal (data not shown).

These finding are presented quantitatively in Fig. 2, in which the cumulative amount of sulforhodamine that was transported across the full-thickness pig skin after microdermabrasion is shown over time. Sulforhodamine permeation in the untreated negative-control skin was low, which is consistent with the histology shown in Fig. 1. The cumulative amount transported after 12 h was $0.010 \pm 0.008\ \mu g/cm^2$.

After skin abrasion that partially removed stratum corneum, sulforhodamine permeation was significantly larger, The cumulative amount transported after 12 h was $0.57 \pm 0.06\ \mu g/cm^2$ (for the −45 kPa, 10 passes data) which is 57 times greater than in the untreated skin. In this case, two different microdermabrasion pressures were used, but both removed similar amounts of tissue (data not shown), indicating that the number of passes (i.e., time of exposure) is more important to determining tissue removal than is the suction pressure.

Microdermabrasion that removed the full stratum corneum increased transdermal transport still more dramatically. The cumulative amount transported after 12 h was $4.31 \pm 0.14\ \mu g/cm^2$ (for the −45 kPa, 50 passes data) which is approximately 7.5 times greater than in the partially abraded skin and approximately 430 times greater than in the untreated skin. In this case, transdermal transport reached steady state during the 12-h experiment, which permitted calculation of a skin permeability of $1.4\times10^{-3} \pm 0.2\times10^{-3}$ cm/h with a lag time of 6.6 ± 1.7 h (for the −45 kPa, 50 passes data). These results are consistent with our expectation that microdermabrasion under conditions that remove stratum corneum can dramatically increase skin permeability to hydrophilic molecules.

Permeation of BSA and Inactivated Influenza Virus—Texas Red-labeled BSA was applied to intact pig skin and, as shown in Fig. 3, BSA did not diffuse significantly into the untreated negative control skin (Figs. 3A – 3C). After complete removal of the stratum corneum, BSA diffused deeply into the skin, especially at the 24 h time point (Figs. 3D – 3F). Histological images collected after delivery of R18-labeled inactivated influenza virus similarly showed that insignificant amounts of the virus permeated into intact skin (Figs. 4A – 4C), but significant delivery was achieved after removal of stratum corneum (Figs. 4D – 4F). This shows that the stratum corneum provided a significant barrier to diffusion of these compounds into the skin, and that microdermabrasion can be used to remove that barrier.

Despite histological evidence for permeation of BSA and inactivated influenza virus into the skin, Franz-cell diffusion measurements over 24 h showed no transdermal delivery above background noise. This is probably because (i) these compounds are much larger than sulforhodamine and therefore diffuse across skin more slowly and (ii) this experiment used full thickness pig skin, which has a thick dermis (2 – 5 mm) that takes time to cross. However, lack of detectable delivery across the dermis may not be problematic for applications, where proteins for systemic administration need to be delivered to capillaries in the superficial dermis and vaccines need to be delivered to resident antigen-presenting cells in epidermis and dermis.

Skin Permeability After Removal of Stratum Corneum Vs. Removal of Full Epidermis in Human Skin

In the next set of experiments, we made a number of changes to the protocol. First, we used split-thickness human skin, which has the advantages of being human rather than animal tissue and of reducing the thickness of dermis that provides an artifactually large barrier when modeling transdermal delivery to superficial dermal capillaries. We also used microdermabrasion conditions that removed stratum corneum and compared their effects to conditions that removed full epidermis. Finally, we placed a polymer mask containing 125-μm holes on the skin surface during microdermabrasion in order to make an array of small holes in the skin, rather than abrading a single, large area. This geometry of skin abrasion better mimics the way the skin barrier is breached in other methods, such as microneedles and thermal ablation, and should be more suitable for future applications of microdermabrasion in transdermal drug delivery.

The histological results from delivery of sulforhodamine in this way are shown in Fig. 5. The left column shows the effects of microdermabrasion under conditions that remove stratum corneum, while the right column shows the effects after removal of full epidermis. The tissue removal pattern enabled by the mask is shown in the en face images of the skin surface presented in the top row of the figure (Figs. 5A – 5B), where the regions of abrasion are colored with a green dye that selectively stains sites of stratum corneum removal. The green-stained spots on the skin with full epidermis removal (Fig. 5B) appear darker and larger, which is consistent with deeper abrasion. The middle row shows representative H&E-stained histological sections of skin showing removal of stratum corneum (Fig. 5C) and full epidermis (Fig. 5D) at spots corresponding to the holes in the masks (see arrows). Finally, the bottom row shows the same histological sections of skin presented in the middle row, but imaged under fluorescence optics to show the permeation of sulforhodamine into the skin after microdermabrasion. Note that there is no sulforhodamine fluorescence at the sites of tissue removal (see arrows), because there is no tissue there to retain the dye during tissue washing.

Permeation of Sulforhodamine—We next quantified skin permeability by measuring the cumulative permeation of sulforhodamine across skin with stratum corneum and full epidermis removed, as shown in Fig. 6. Sulforhodamine did not significantly penetrate intact skin. The cumulative amount transported after 12 h was below the detection limit.

Removing the stratum corneum significantly increased the flux. The cumulative amount transported after 12 h was 7.4 ± 0.3 $\mu g/cm^2$. The corresponding skin permeability calculated from the steady-state region of the graph was $1.2\times10^{-3} \pm 0.7\times10^{-3}$ cm/h with a lag time of 0.78 ± 0.46 h, which is a similar permeability to that found in pig skin, but with a shorter lag time due to the decreased thickness of the dermatomed skin.

Removing full epidermis increased skin permeability even further. The cumulative amount transported after 12 h was 56.5 ± 0.2 $\mu g/cm^2$, and the corresponding skin permeability was $8.7\times10^{-3} \pm 1.2\times10^{-3}$ cm/h with a lag time of 0.32 ± 0.11 h. Skin permeability of sulforhodamine was approximately 7 times higher after removal of full epidermis compared to removal of stratum corneum. This shows that the viable epidermis was a significant barrier to transdermal diffusion of sulforhodamine after removal of stratum corneum.

Permeation of Insulin—We also assessed skin permeability to insulin after microdermabrasion using an FDA-approved human insulin solution (U-500 Humulin) spiked with FITC-labeled bovine insulin. Skin permeability was determined by measuring transdermal flux of FITC-labeled insulin by fluorescence spectroscopy and FDA-approved insulin by ELISA As shown by the data generated by fluorescence measurements in Fig. 7A,

insulin did not significantly permeate across intact skin. The skin with stratum corneum removed had a permeability to insulin of $2.2\times10^{-5} \pm 3.7\times10^{-6}$ cm/h with a lag time of 2.0 ± 1.6 h. The skin with full epidermis removed had a permeability to insulin of $2.4\times10^{-4} \pm 1.2\times10^{-4}$ cm/h with a lag time of 7.2 ± 0.9 h. The skin permeability to insulin after removal of full epidermis was approximately 11 times higher than in skin with only stratum corneum removed.

Similar data were generated by measuring insulin flux by ELISA (Fig. 7B). Using this assay, the skin with stratum corneum removed had an insulin permeability of $4{,}5\times10^{-6} \pm 4.9\times10^{-6}$ cm/h with a lag time of 9.5 ± 2.9 h. The skin with full epidermis removed had an insulin permeability of $5.0\times10^{-4} \pm 2.2\times10^{-4}$ cm/h with a lag time of 6.7 ± 1.8 h. The skin permeability to insulin after removal of full epidermis was more than 100 times higher than in skin with only stratum corneum removal.

There is generally good agreement between the measurements made by the fluorescence and ELISA assays for skin with full epidermis removed. The values for skin with only stratum corneum removed do not agree, where the fluorescence-based assay yielded a much higher permeability and shorter lag time than the corresponding measurements by ELISA. We expect the ELISA assay is more reliable because ELISA is highly specific to insulin detection and because the lag time is surprisingly short for the fluorescence data.

DISCUSSION

This study primarily sought to assess the relative barrier properties of stratum corneum and viable epidermis. As novel physical and chemical methods are developed that effectively permeabilize stratum corneum, the role of the barrier posed by viable epidermis becomes increasingly important. Our data suggest that methods that only permeabilize stratum corneum are much less effective than those that permeabilize the full epidermis. We found that removal of stratum corneum dramatically increased skin permeability, but removal of the full epidermis increased skin permeability by another 1 – 2 orders of magnitude beyond the skin permeability achieved with just stratum corneum removed, depending on the molecule being delivered.

Relevance of study findings to design of drug delivery methods

These findings are significant to development of novel methods of transdermal drug delivery. For example, chemical approaches have emphasized formulations that selectively disrupt lipid bilayer structures in the stratum corneum and typically seek specifically to avoid effects in the viable epidermis in order to prevent skin irritation (4, 5). This study suggests that such approaches are inherently limited as they increase stratum corneum permeability but do not address the barrier of the full epidermis.

Design of physical approaches can also be improved by the findings of this study. For example, thermal ablation using lasers and heating elements can be controlled to remove different amounts of skin tissue (21–24). This study suggests that more-aggressive ablation will be more effective. Recent studies that measured skin permeability after removing different amounts of skin tissue by thermal ablation showed that permeation of diclofenac increased with increasing pore depth into epidermis for diclofenac (25), but not for lidocaine (26).

Microneedles do not typically remove tissue, but instead puncture holes into the skin (27). This study suggests that microneedles that penetrate only across stratum corneum should be less effective than ones that penetrate more deeply to create holes that cross the full epidermis. Due to the biomechanics of microneedle insertion into skin, it is difficult to insert

microneedle just across stratum corneum and not across the full epidermis (28). As a result, most studies have used microneedles that penetrate more deeply, which may contribute to their success in drug delivery. A notable exception involves extremely short microneedles inserted under high velocity, which are reported to penetrate into, but not across, the epidermis (29). However, these studies addressed skin vaccination, where the target cells were dendritic cells found in the epidermis and delivery to the dermis to reach systemic circulation was not needed.

The reason why some studies have emphasized limiting permeabilizing effects to stratum corneum is because damaging viable epidermis could cause pain, irritation and other adverse effects. Our study conducted in vitro cannot assess these possible limitations. However, in a previous study we used similar microdermabrasion conditions to remove skin tissue in vivo in guinea pigs and monitored skin repair (30). We found that microdermabrasion that removed stratum corneum was well tolerated by the animals and that skin histology returned to normal appearance within 24 h. In a related body of literature, we and others have found that insertion of microneedles across the full epidermis and into the dermis is reported as painless, generates only mild, transient erythema and is otherwise well tolerated in human subjects (31–33). Similarly, thermal ablation of skin that is believed to remove viable epidermis has also been well tolerated (23, 34).

This study was carried out in vitro, which has limitations. For example, when we use the term “viable epidermis,” we recognize that the epidermis is no longer living in the cadaver skin used in this study, but use the term to identify the portion of epidermis located below the stratum corneum, following common convention (2). However, we previously conducted a study of insulin delivery to diabetic rats in vivo after microdermabration of the skin. In that study, we similarly found that insulin delivery, and corresponding blood glucose reduction, were much larger after removal of full epidermis than after removal of just stratum corneum. Moreover, there is growing evidence for the presence of tight junctions in the viable epidermis that limit diffusion of molecules (3). These tight junctions are probably not intact in cadaver skin, which suggests that our in vitro studies may underestimate the barrier properties of viable epidermis in vivo. Another component of the epidermal barrier is the basal lamina, located between the viable epidermis and dermis, which has been shown to serve as a barrier to compounds larger than 40 kDa (35), but, on the other hand, is sufficiently permeable to allow migration of cells, such as Langerhans cells, between the epidermis and dermis (2).

Results from this study are generally consistent with the prior literature. A previous study compared glucose transport in dermis versus viable epidermis and concluded that glucose diffusivity was much lower in the viable epidermis compared to the dermis (36). Much lower diffusivities of steroids in tape-stripped skin measured in one study (37) compared to their diffusivities in the dermis measured in another study (38) would be explained by lower diffusivity in viable epidermis compared to dermis (38).

Microdermabrasion as a drug delivery method

Although the primary focus of this study used microdermabrasion as a tool to examine barrier properties of stratum corneum and viable epidermis, our secondary goal was to assess the use of microdermabrasion as a skin pretreatment to increase transdermal drug delivery. This study showed that a brief (< 1 min) pretreatment of skin dramatically increased skin permeability of a small hydrophilic molecule (sulforhodamine), proteins (BSA, insulin) and a vaccine (inactivated influenza virus). The ability to deliver hydrophilic compounds and macromolecules would dramatically expand the scope of molecules that can be delivered across skin and could provide a useful alternative to hypodermic injection of vaccines and protein therapeutics.

Our approach to microdermabrasion enabled three-dimensional control of the amount of tissue removed. Controlling microdermabrasion parameters – especially the number of passes, which controlled the duration of exposure – controlled the depth of tissue removal. The use of a mask on the skin surface controlled the area of tissue removal, which was limited to a circle of 125 μm diameter in this study. This hole size is similar to those created by thermal ablation and microneedles, which have been well tolerated in animals and humans (23, 31–34). In this way, microdermabrasion removed microscopically small pieces of tissue, each with a volume of just 1.2×10^{-6} cm^3 (based on diameter of 125 μm and a depth of 100 μm). This is expected to be painless, rapidly healing, and almost invisible to the eye.

Current microdermabrasion instruments used for cosmetic purposes are relatively large and costly, and require expertise to operate, which would limit use primarily to in-clinic procedures. However, we envision home-use of microdermabrasion by patients themselves by replacing current multi-user devices that include multiple adjustable controls with simpler devices purpose-built to increase skin permeability. Hand-held, potentially single-use, devices could be developed specifically for skin tissue removal at predetermined operating conditions. Future research will be needed to assess the possibility of developing such a small, simple-to-operate and low-cost device.

CONCLUSION

Most approaches to increasing skin permeability seek to breach the stratum corneum barrier without damaging viable epidermis. However, we hypothesized that viable epidermis offers a significant permeability barrier to both small molecules and macromolecules that becomes the rate-limiting step upon sufficient permeabilization of the stratum corneum. This study supported that hypothesis by showing that after significantly increasing skin permeability by removing stratum corneum using controlled microdermabrasion, skin permeability was further increased by 1 – 2 orders of magnitude to a small hydrophilic molecule as well as macromolecules upon removal of the full epidermis.

These observations lead to the following three conclusions: (i) viable epidermis poses a significant barrier to transdermal diffusion in the absence of stratum corneum, (ii) transdermal drug delivery using methods that significantly increase stratum corneum permeability, such as certain chemical formulations, thermal ablation, microneedles and microdermabrasion, may benefit from increasing permeability of the full epidermis and not just the stratum corneum and (iii) microdermabrasion, especially in combination with a mask to limit the area of tissue removed, may be a novel and effective means of increasing skin permeability for transdermal delivery of hydrophilic drugs and macromolecules.

Acknowledgments

We would like to thank Dr. Yeu-Chun Kim for supplying and preparing the fluorescently labeled influenza virus; Dr. Jeong-Woo Lee and Aritra Sengupta for advice on the sulforhodamine diffusion experiments; and Donna Bondy for administrative support. This work was carried out in the Center for Drug Design, Development and Delivery and the Institute for Bioengineering and Bioscience at Georgia Tech with financial support in part from the National Institutes of Health.

Mark Prausnitz serves as a consultant and is an inventor on patents licensed to companies developing microneedle-based products.

REFERENCES

1. Prausnitz MR, Langer R. Transdermal drug delivery. Nat Biotechnol. 2008; 26:1261–1268. [PubMed: 18997767]

2. Bolognia, J.; Jorizzo, J.; Schaffer, J. Dermatology. Saunders; Philadelphia: 2012.
3. Kirschner N, Houdek P, Fromm M, Moll I, Brandner JM. Tight junctions form a barrier in human epidermis. Eur J Cell Biol. 2010; 89:839–842. [PubMed: 20732726]
4. Karande P, Jain A, Ergun K, Kispersky V, Mitragotri S. Design principles of chemical penetration enhancers for transdermal drug delivery. P Natl Acad Sci USA. 2005; 102:4688–4693.
5. Smithand, E.; Maibach, H. Percutaneous Penetration Enhancers. CRC Press; Boca Raton, FL: 2005.
6. Karande P, Jain A, Mitragotri S. Discovery of transdermal penetration enhancers by high-throughput screening. Nat Biotechnol. 2004; 22:192–197. [PubMed: 14704682]
7. Kim YC, Ludovice PJ, Prausnitz MR. Transdermal delivery enhanced by magainin pore-forming peptide. J Control Release. 2007; 122:375–383. [PubMed: 17628164]
8. Polat BE, Hart D, Langer R, Blankschtein D. Ultrasound-mediated transdermal drug delivery: mechanisms, scope, and emerging trends. J Control Release. 2011; 152:330–348. [PubMed: 21238514]
9. Arora A, Prausnitz MR, Mitragotri S. Micro-scale devices for transdermal drug delivery. Int J Pharm. 2008; 364:227–236. [PubMed: 18805472]
10. Fujimoto T, Shirakami K, Tojo K. Effect of microdermabrasion on barrier capacity of stratum corneum. Chem Pharm Bull. 2005; 53:1014–1016. [PubMed: 16079538]
11. Karimipour DJ, Kang S, Johnson TM, Orringer JS, Hamilton T, Hammerberg C, Voorhees JJ, Fisher G. Microdermabrasion with and without aluminum oxide crystal abrasion: a comparative molecular analysis of dermal remodeling. J Am Acad of Derm. 2006; 54:05–410.
12. Lew BL, Cho Y, Lee MH. Effect of serial microdermabrasion on the ceramide level in the stratum corneum. Dermatol Surg. 2006; 32:376–379. [PubMed: 16640682]
13. Bhallaand M, Thami G. Microdermabrasion: reappraisal and brief review of literature. Dermatol Surg. 2006; 32:809–814. [PubMed: 16792646]
14. Freedman BM, Rueda-Pedraza E, Earley RV. Clinical and histologic changes determine optimal treatment regimens for microdermabrasion. J Dermatol Treat. 2002; 13:193–200.
15. Andrews SN, Lee JW, Choi SO, Prausnitz MR. Transdermal insulin delivery using microdermabrasion. Pharm Res. 2011; 28:2110–2118. [PubMed: 21499837]
16. Fang JY, Lee WR, Shen SC, Fang YP, Hu CH. Enhancement of topical 5-aminolaevulinic acid delivery by erbium : YAG laser and microdermabrasion: a comparison with iontophoresis and electroporation. Br J Dermatol. 2004; 151:132–140. [PubMed: 15270882]
17. Lee WR, Shen SC, Wang KH, Hu CH, Fang JY. Lasers and microdermabrasion enhance and control topical delivery of vitamin C. J Invest Dermatol. 2003; 121:1118–1125. [PubMed: 14708614]
18. Lee WR, Tsai RY, Fang CL, Liu CJ, Hu CH, Fang JY. Microdermabrasion as a novel tool to enhance drug delivery via the skin: An animal study. Dermatol Surg. 2006; 32:1013–1022. [PubMed: 16918563]
19. Andrews SN, Zarnitsyn V, Bondy B, Prausnitz MR. Optimization of microdermabrasion for controlled removal of stratum corneum. Int J Pharm. 2011; 407:95–104. [PubMed: 21272628]
20. Koutsonanos DG, Martin MD, Zarnitsyn VG, Sullivan SP, Compans RW, Prausnitz MR, Skountzou I. Transdermal influenza immunization with vaccine-coated microneedle arrays. Plos One. 2009; 4
21. Jacques SL, McAuliffe DJ, Blank IH, Parrish JA. Controlled removal of human stratum-corneum by pulsed laser. J Invest Dermatol. 1987; 88:88–93. [PubMed: 3794393]
22. Sintov AC, Krymberk I, Daniel D, Hannan T, Sohn Z, Levin G. Radiofrequency-driven skin microchanneling as a new way for electrically assisted transdermal delivery of hydrophilic drugs. J Control Release. 2003; 89:311–320. [PubMed: 12711453]
23. Badkar AV, Smith AM, Eppstein JA, Banga AK. Transdermal delivery of interferon alpha-2B using microporation and iontophoresis in hairless rats. Pharm Res. 2007; 24:1389–1395. [PubMed: 17443396]
24. Lee JW, Gadiraju P, Park JH, Allen MG, Prausnitz MR. Microsecond thermal ablation of skin for transdermal drug delivery. J Control Release. 2011; 154:58–68. [PubMed: 21596072]

25. Bachhav YG, Heinrich A, Kalia YN. Using laser microporation to improve transdermal delivery of diclofenac: increasing bioavailability and the range of therapeutic applications. Eur J Pharm Biopharm. 2011; 78:408–414. [PubMed: 21397689]
26. Bachhav YG, Summer S, Heinrich A, Bragagna T, Bohler C, Kalia YN. Effect of controlled laser microporation on drug transport kinetics into and across the skin. J Control Release. 2010; 146:31–36. [PubMed: 20678988]
27. Kim YC, Park JH, Prausnitz MR. Microneedles for drug and vaccine delivery. Adv Drug Deliver Rev. 2012 in press.
28. Crichton ML, Ansaldo A, Chen XF, Prow TW, Fernando GJP, Kendall MAF. The effect of strain rate on the precision of penetration of short densely-packed microprojection array patches coated with vaccine. Biomaterials. 2010; 31:4562–4572. [PubMed: 20226519]
29. Fernando GJP, Chen XF, Prow TW, Crichton ML, Fairmaid EJ, Roberts MS, Frazer IH, Brown LE, Kendall MAF. Potent immunity to low doses of influenza vaccine by probabilistic guided micro-targeted skin delivery in a mouse model. Plos One. 2010; 5
30. Andrews SN, Lee JW, Prausnitz MR. Recovery of skin barrier after stratum corneum removal by microdermabrasion. AAPS Pharmscitech. 2011; 12:1393–1400. [PubMed: 22009306]
31. Gill HS, Denson DD, Burris BA, Prausnitz MR. Effect of microneedle design on pain in human volunteers. Clin J Pain. 2008; 24:585–594. [PubMed: 18716497]
32. Pettisand RJ, Harvey AJ. Microneedle delivery: clinical studies and emerging medical applications. Ther Deliv. 2012; 3:357–371. [PubMed: 22833995]
33. Hoesly FJ, Borovicka J, Gordon J, Nardone B, Holbrook JS, Pace N, Ibrahim O, Bolotin D, Warycha M, Kwasny M, West D, Alam M. Safety of a novel microneedle device applied to facial skin: a subject- and rater-blinded, sham-controlled, randomized trial. Arch Dermatol. 2012 In press.
34. Levin G, Gershonowitz A, Sacks H, Stern M, Sherman A, Rudaev S, Zivin I, Phillip M. Transdermal delivery of human growth hormone through RF-microchannels. Pharm Res. 2005; 22:550–555. [PubMed: 15846462]
35. Bissett, D. Ch 3: Anatomy and Biochemistry of Skin. In: Kydonieus, AF.; Berner, B., editors. Transdermal delivery of drugs. Vol. Vol. I. CRC Press, Inc.; 1987. p. 160
36. Khalil E, Kretsos K, Kasting GB. Glucose partition coefficient and diffusivity in the lower skin layers. Pharm Res. 2006; 23:1227–1234. [PubMed: 16715366]
37. Tojo K, Chiang CC, Chien YW. Drug permeation across the skin - effect of penetrant hydrophilicity. J Pharm Sci. 1987; 76:123–126. [PubMed: 3572749]
38. Kretsos K, Miller MA, Zamora-Estrada G, Kasting GB. Partitioning, diffusivity and clearance of skin permeants in mammalian dermis. Int J Pharm. 2008; 346:64–79. [PubMed: 17703903]

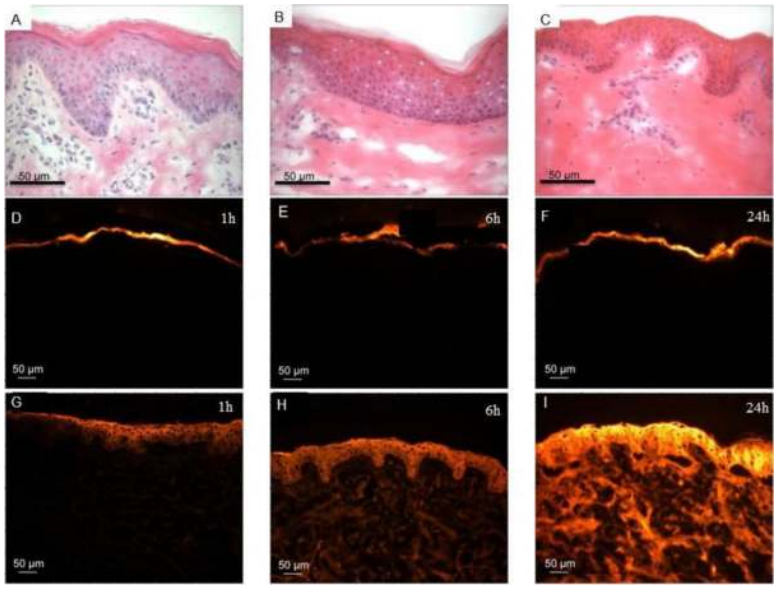

Figure 1.

Representative histological sections of porcine skin showing permeation of red-fluorescent sulforhodamine into skin after tissue removal using microdermabrasion. The top row shows hematoxylin- and eosin-stained skin illustrating the degree of tissue removal: (A) unabraded negative control, (B) partial removal of stratum corneum (microdermabrasion at −45 kPa and 10 passes) and (C) complete removal of stratum corneum (microdermabrasion at −45 kPa and 50 passes). The middle row shows unabraded skin at 1 h (D), 6 h (E) and 24 h (F) after applying sulforhodamine to the skin surface. The bottom row shows abraded skin with complete stratum corneum removal at 1 h (G), 6 h (H) and 24 h (I) after applying sulforhodamine to the skin surface. All fluorescence microscopy images (D–I) were collected at the same exposure time and gain using the same microscope and camera.

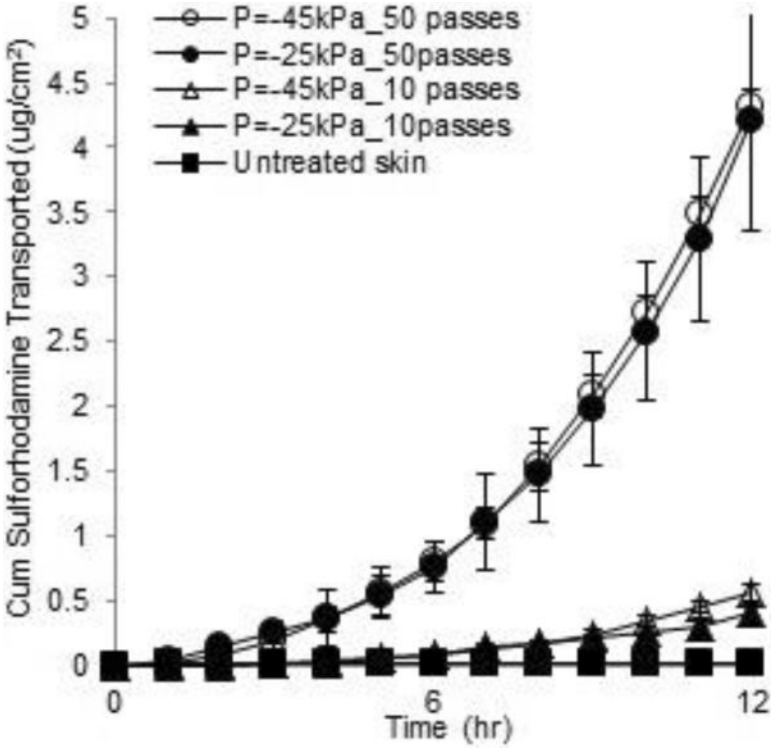

Figure 2.

The cumulative permeation of sulforhodamine across full-thickness porcine skin after tissue removal by microdermabrasion: unabraded negative control skin (■), skin with partial stratum corneum removal abraded at −25 kPa (▲) and −45 kPa (Δ) with 10 passes, and skin with full stratum corneum removal abraded at −25 kPa (●) and −45 kPa (◯) with 50 passes. Each data point represents the average ± standard deviation (SD) of n=3 replicates.

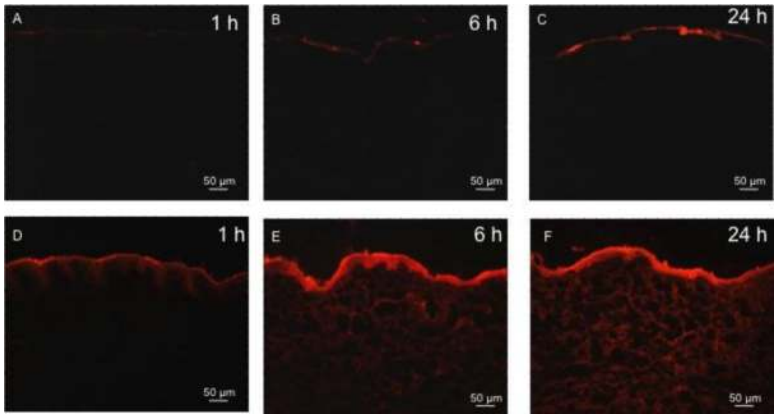

Figure 3.

Representative histological sections of porcine skin showing permeation of red-fluorescent Texas Red-labeled bovine serum albumin (BSA) into skin after tissue removal using microdermabrasion. The top row shows unabraded skin at 1 h (A), 6 h (B) and 24 h (C) after applying BSA to the skin surface. The bottom row shows abraded skin with complete stratum corneum removal (microdermabrasion at −50 kPa, 50 passes) at 1 h (D), 6 h (E) and 24 h (F) after applying BSA to the skin surface. All images were collected at the same exposure time and gain using the same microscope and camera.

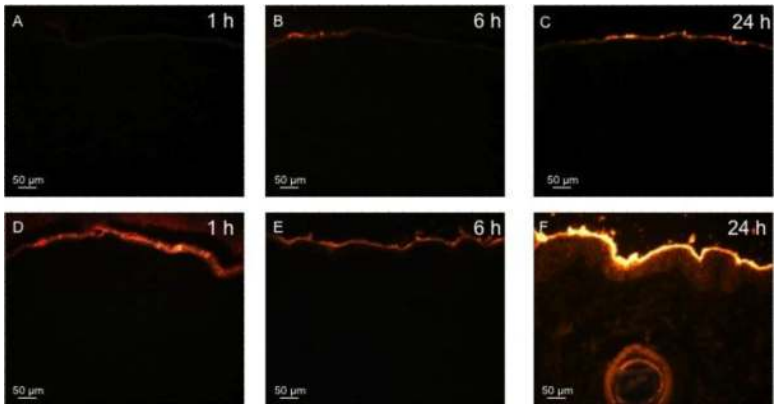

Figure 4.

Representative histological sections of porcine skin showing permeation of red-fluorescent R-18-labeled inactivated influenza virus into skin after tissue removal by microdermabrasion. The top row shows unabraded skin at 1 h (A), 6 h (B), and 24 h (C) after applying influenza virus to the skin surface. The bottom row shows abraded skin with complete stratum corneum removal (microdermabrasion at −50 kPa, 50 passes) at 1 h (D), 6 h (E), and 24 h (F) after applying influenza virus to the skin surface. All images were collected at the same exposure time and gain using the same microscope and camera.

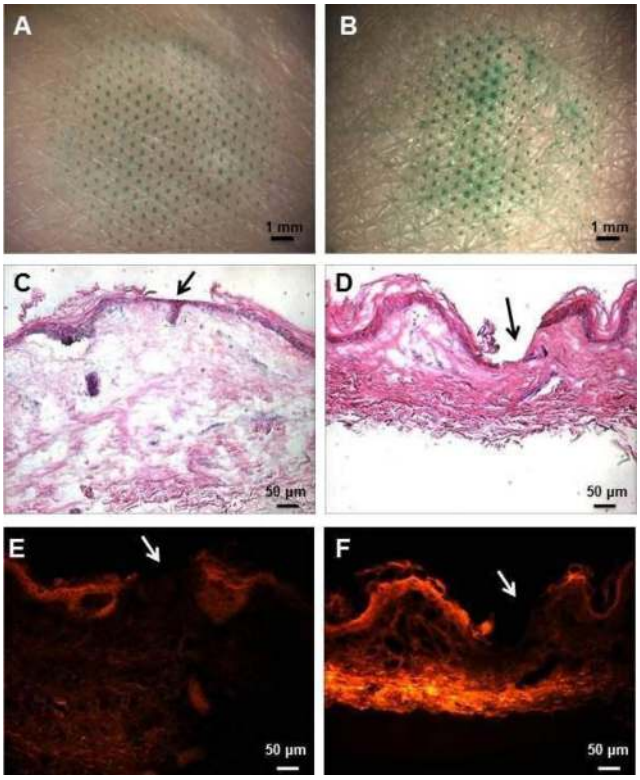

Figure 5.
Representative images of split-thickness human skin after microdermabrasion through a mask applied to the skin surface to control tissue removal in three dimensions. The left column shows skin abraded to remove the stratum corneum (microdermabrasion at −30 kPa for 20 s) and the right column shows skin abraded to remove full epidermis (microdermabrasion at −50 kPa for 60 s). The sites of tissue removal as determined by the mask geometry are shown by staining with green dye in the en face images shown in the top row (A, B). The depth of tissue removal at the sites of microdermabrasion is shown in the histological sections with H&E staining in the middle row, where stratum corneum was removed (C) and full epidermis was removed (D). The arrows point to the areas of abrasion. Finally, the same histological sections shown in parts (C) and (D) are shown again using fluorescence optics (E, F). The permeation of sulforhodamine into the skin is seen after sulrorhodamine had been applied to the skin surface for 12 h.

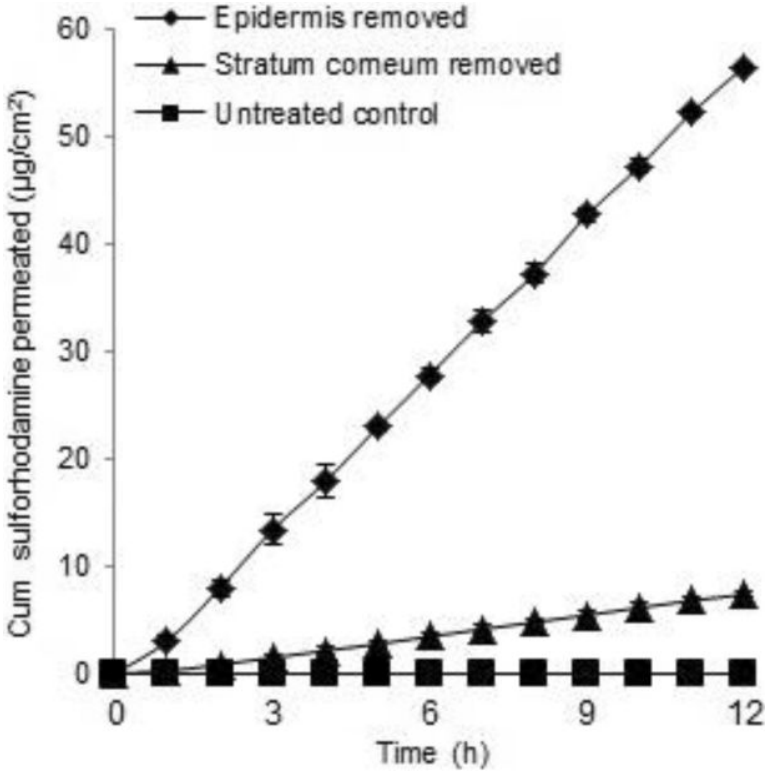

Figure 6.
The cumulative permeation of sulforhodamine across split-thickness human skin after tissue removal by microdermabrasion through a mask: unabraded skin (□), skin with stratum corneum removed by microdermabrasion at −30 kPa for 20 s (▲) and skin with full epidermis removed by microdermabrasion at −50 kPa for 60 s (◆). Average ± SD, n= 3.

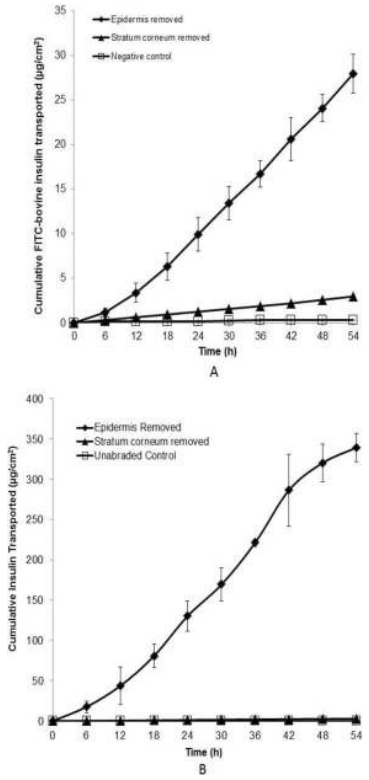

Figure 7.

The cumulative permeation of insulin across split-thickness human skin after tissue removal by microdermabradsion through a mask: unabraded skin (□), skin with stratum corneum removed by microdermabrasion at −30 kPa for 20 s (▲) and skin with full epidermis removed by microdermabrasion at −50 kPa for 60 s (◆). (A) Insulin delivery was determined by spectrofluorimetry based on permeation of FITC-labeled bovine insulin. (B) Insulin delivery was determined by ELISA based on permeation of recombinant human insulin (U-500 Humulin). Average ± SD, n= 3. Permeation of insulin in (B) is greater than in (A) because the human insulin was provided at a higher concentration than the bovine insulin in the donor solution (see Materials and Methods).